

# MACRO-MODEL INDEPENDENT MIGRATION TO ZERO OFFSET (CRS-MZO)

G. Garabito, W. Söllner and J. C. Cruz

**email:** *german@ufpa.br*

**keywords:** *Coherency; Optimization; Stacking*

## ABSTRACT

*The Common-Reflection-Surface (CRS) stack is a well-established time imaging method that provides high-quality stacking of three or two dimensional multicoverage seismic data, and also important kinematic wavefield attributes. The CRS stack method has been used successful to simulate zero-offset (ZO) seismic sections, providing high-resolution ZO seismic section even for complex geologic structures. The Migration to ZO (MZO) is a method to transform a common-offset (CO) into a ZO data through an imaging or mapping procedure. In this paper, we present a new methodology to obtain a migration to zero-offset (MZO) by using the CRS traveltime formula and the optimized CRS stack parameters, namely the emergence angle of the normal ray, and the radius of curvature of the normal incidence point (NIP) wave. It is so called CRS-MZO and takes advantage of the fact that unlike the normal-moveout (NMO) method, the CRS stack is not restricted to common-midpoint (CMP) gathers, but it uses large supergathers of arbitrary source-receiver configuration, without requirement of event selections by the interpreter. Unlike the conventional MZO that needs a velocity model to transform the data, the CRS-MZO is velocity model independent. The proposed CRS-MZO method has been validated using the 2D Marmousi synthetic data and finally applied to 2D land seismic data of the Tacutu Basin (Brazil).*

## INTRODUCTION

The Common Reflection Surface (CRS) stack method was developed to construct stacked zero-offset (ZO) sections from multicoverage seismic data. In addition, the CRS-MZO method produce two sections of CRS attributes and one coherency section. The CRS is a data-driven method, i.e., it does not require an a priori known velocity model. By applying optimization techniques the CRS method estimates automatically the needed stacking parameters. The CRS method was presented for the first time by Müller (1998). However, the CRS parameter search strategy used to produce the results shown in that paper was only explained in Müller (1999). By Müller's search strategy, the initial three CRS parameters are estimated by one-parametric search performed on CMP and ZO stacked sections. The final search of the CRS parameters is done in the multicoverage data domain by using the Nelder-Mead optimization algorithm. Other contributions in the development of optimization strategies for estimating the CRS parameters can be found in Birgin et al. (1999); Mann (2001); Jäger et al. (2001) and Garabito et al. (2001).

In the CRS method the stacking curves are defined by a hyperbolic approximation of the reflection traveltime in midpoint and half-offset coordinates. The so-called CRS stacking operator is parameterized by three kinematic wavefield-attributes useful for several seismic applications, and in the present 2D situation, depends on three parameters: the emergence angle of the normal ray,  $\beta_o$ , and the radii of curvature  $R_{NIP}$  and  $R_N$  of two hypothetical wavefronts, so-called Normal-Incidence-Point (NIP) wave and Normal (N) wave, respectively. Both wavefronts are related to second-order paraxial approximations of the reflection traveltime (Hubral and Krey, 1980). The CRS stacking surface is a second-order reflection traveltime Taylor expansion in offset and midpoint domain, of the true reflection traveltime in the vicinity of a normal

(zero-offset) ray. The CRS stack formalism has been extended to include situations for a central ray of finite-offset (Zhang et al., 2001), topography and near-surface inhomogeneity effects (Chira-Oliva et al., 2001).

By using a stratified model with homogeneous layers separated by curved interfaces, Jäger et al. (2001) showed the validity of the CRS stack method to simulate the ZO section and to determine the kinematic wavefield attributes from the multicoverage data.

In this paper, based on a diffraction traveltime approximation obtained from the hyperbolic reflection traveltime or so-called CRS stacking operator, we build a new migration to zero offset (CRS-MZO) method to simulate ZO (stacked) sections from pre-stack multicoverage data. The CRS-MZO operator is defined in the present 2D situation by two CRS parameters: the emergence angle of the normal ray,  $\beta_o$ , and the radius of curvature,  $R_{NIP}$ , of the hypothetical wavefront, so-called Normal-Incidence-Point (NIP) wave. These two parameter values are automatically determined by an one-step search approach from the full pre-stack data. We employ a simulated annealing (SA) algorithm, see e.g. Kirkpatrick et al. (1983) and Corana et al. (1987), as a global optimization scheme to estimate the CRS-MZO parameters. Similar to the conventional CRS approach of Jäger et al. (2001), we obtain a CRS-MZO stack section, as well as three additional sections, namely the sections of maximum coherence values, emergence angles  $\beta_o$ , and radius of curvature  $R_{NIP}$ , respectively.

To exemplify the main steps of the CRS-MZO approach, we use a simple synthetic model with three homogeneous layers separated by smooth interfaces. On the other hand, to evaluate the image quality and the robustness of the CRS-MZO algorithm, we present applications of the Marmousi dataset in comparison with NMO/DMO. Finally, we present a real data application of the Tacutu Basin, which is localized at the border between the Roraima State (Brazil) and the Rupununi District (Guiana Cooperative Republic).

### CRS STACK TRAVELTIME APPROXIMATIONS

We start by reviewing the CRS method formalism as given by Jäger et al. (2001). The 2-D CRS stack hyperbolic second-order Taylor expansion can be derived by means of paraxial ray theory (Schleicher et al. (1993)). It approximates the finite-offset reflection traveltime in the vicinity of a fixed normal ray, generally called a central ray, that is specified by its emergence point,  $x_0$ , called the central point and generally taken as a certain CMP along the seismic profile. The two-way traveltime of the ZO central ray that pertains to  $x_0$  is denoted  $t_0$ . A given point,  $P_0 = (x_0, t_0)$  in the output ZO section is constructed by stacking along the following CRS traveltime curve (Tygel et al., 1997)

$$t^2(x_m, h) = \left[ t_0 + \frac{2 \sin \beta_0}{v_0} (x_m - x_0) \right]^2 + \frac{2t_0 \cos^2 \beta_0}{v_0} \left[ \frac{(x_m - x_0)^2}{R_N} + \frac{h^2}{R_{NIP}} \right]. \quad (1)$$

As indicated above,  $x_0$  and  $t_0$  denote the emergence point of the normal ray on the seismic line, the central point, and its ZO traveltime, respectively;  $x_m$  and  $h$  are midpoint and half-offset coordinates:  $x_m = (x_s + x_r)/2$  and  $h = (x_s - x_r)/2$ , where  $x_s$  and  $x_r$  are the coordinates of the source and receiver on a planar acquisition surface.

The seismic line is considered to coincide with the horizontal Cartesian coordinate axis,  $x$ , along which  $x_s$ ,  $x_r$  and  $x_0$  are specified. The point  $P_0(x_0, t_0)$  in the ZO section to be simulated is the one in which is assigned the stacked seismic amplitudes with formula (1).

In the case that the reflector element collapses into a diffractor point, the NIP and Normal wavefronts coincide. As a consequence,  $R_{NIP} = R_N$ , and the formula (1) reduces to

$$t^2(x_m, h) = \left[ t_0 + \frac{2 \sin \beta_0}{v_0} (x_m - x_0) \right]^2 + \frac{2t_0 \cos^2 \beta_0}{v_0} \left[ \frac{(x_m - x_0)^2 + h^2}{R_{NIP}} \right]. \quad (2)$$

The traveltime approximation from equation 2, called Common-Diffraction-Surface (CDS) stack operator, was used to simultaneously estimate the two parameters  $\beta_0$  and  $R_{NIP}$ , as a first step of the CRS parameter estimation strategy (Garabito et al., 2001). In this work, the pair of CRS parameters ( $\beta_0, R_{NIP}$ ) will be referred as NIP-wave parameters.

In Hubral et al. (1999) was presented a first comparison between the CRS stack and the pre-stack Kirchhoff migration operator. Also, in Jäger et al. (2001) the CRS operator (equation 1), for  $R_{NIP} = R_N$ ,

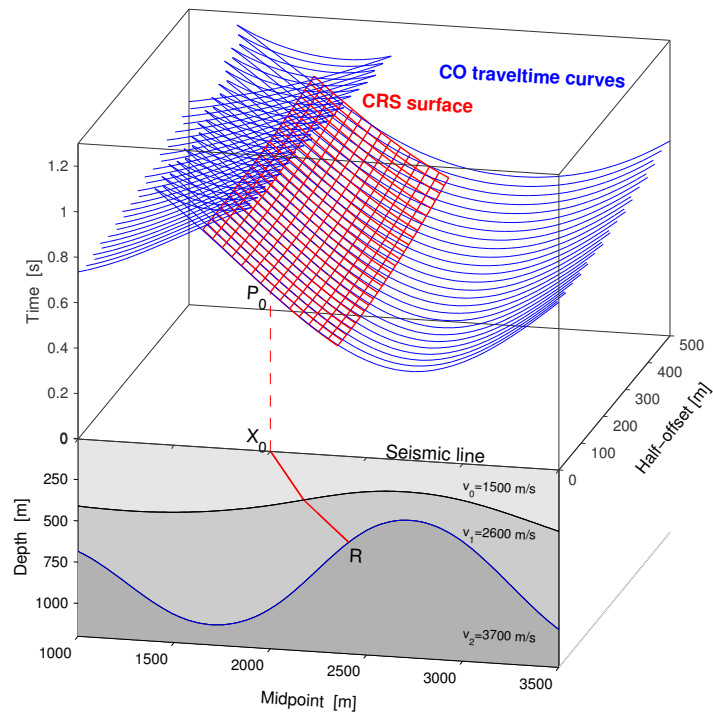


**Figure 1:** The blue curves are common-offset reflection traveltimes for the second reflector. In red is the CRS stack traveltime surface for point  $P_0$  in the ZO seismic section. The lower part is the model with two homogeneous layers above a half-space separated by a curved interface.

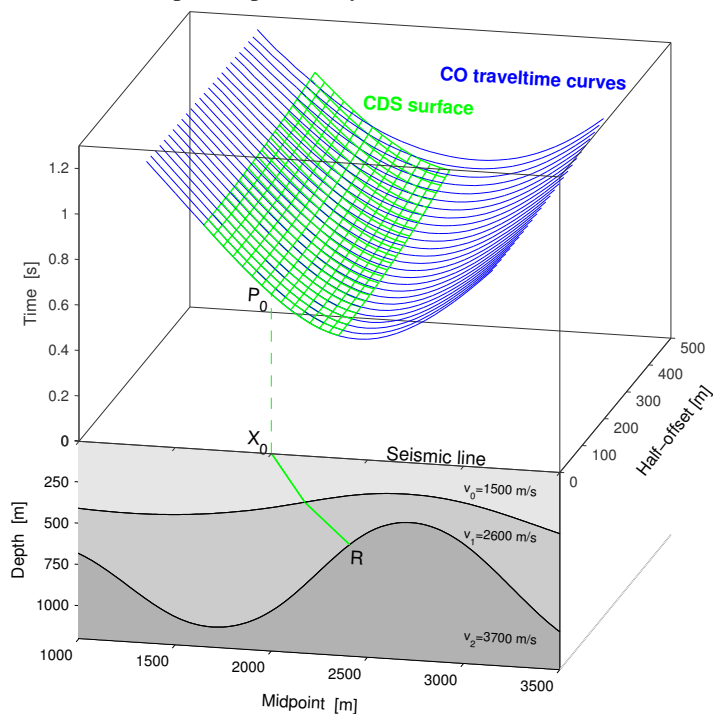


**Figure 2:** The blue surface is the Kirchhoff operator for the diffraction point  $R$  over second reflector. The green is the CDS stack traveltime surface for point  $P_0$  in the ZO seismic section. The lower part is the model with two homogeneous layers above a half-space separated by curved interfaces.

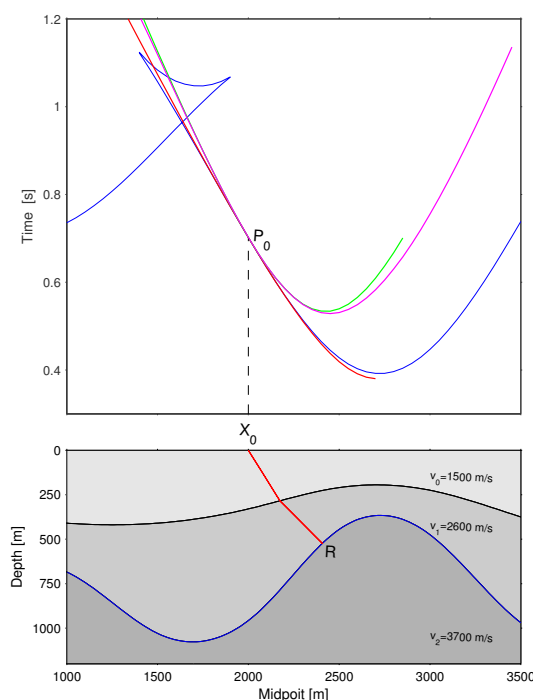


**Figure 3:** In the upper part, the blue line is the ZO reflection traveltimes and the red line is the CRS stack operator related to point  $P_0$ . The magenta line is the ZO Kirchhoff operator and green line is the CDS stack operator related to point  $P_0$  and diffraction point  $R$ , located on the second reflector of the model in the lower part.

was compared with the Kirchhoff operator. Following these concepts, in Mann et al. (2000) was presented an application of the traveltimes approximation (equation 2) for an approximate pre-stack time migration, while Garabito et al. (2006) used the same formula (equation 2) to get a post-stack Kirchhoff type depth migration.

This second-order CDS stack traveltimes curve is now used to simultaneously estimate the two parameters  $\beta_0$  and  $R_{NIP}$ , and apply a limited aperture CRS-MZO.

For a simple model of two homogeneous layers and continuous curved interfaces, Figure 1 depicts the CRS stack traveltimes (CRS surface) and the multicoverage reflection traveltimes, as common-offset (CO) traveltimes curves in the  $(x_m, h, t)$ -domain. Figure 2 depicts the corresponding CDS stack traveltimes, the CRS-MZO operator from equation 2, and the Kirchhoff operator for the same reflection point  $R$  of Figure 1. The CRS and CRS-MZO stacking aperture is a region in the  $(x_m, h)$ -plane in the vicinity of the central ray position  $(x_0, 0)$ . This is also the region where the estimation procedure is performed to find the CRS stacking parameters.

In Figures 1 and 2 the blue curves are CO traveltimes of primary reflections related to the bottom reflector in the model and the central ray Kirchhoff operators, respectively. These curves were calculated by ray tracing and here they are referred as modelled traveltimes. The red lines in Figure 1 are the CRS stack traveltimes and the green lines in Figure 2 are the CDS stack traveltimes. The former approximate the reflection times, calculated from equation 1, and the later approximate the diffraction times calculated from equation 2. In the vicinity of two-way traveltimes  $P_0$  of the central ray both approaches fit very well the modelled CO traveltimes. Hence, the CRS traveltimes surface using equation 2 is a valuable representation for does time imaging steps which assume diffraction points at the endpoint of the central rays Garabito et al. (2001).

Equation 2 can be simplified for the ZO configuration by setting the condition  $h = 0$ . Then, for the ZO plane shown in Figure 3, the blue line represents the reflection traveltimes of the second reflector and the magenta line represents the diffraction traveltimes of a diffraction point at  $R$  on the second reflector. For

the point  $P_0$ , related to the central ray with normal incidence in  $R$  on the second reflector and emerging point  $x_0$ , the CRS operator is shown in red and the CDS operator in green. Again, we observe that also the reduced CDS operator is a good approximation of the corresponding ZO Kirchhoff-type operator, just as the reduced CRS operator approximates the ZO reflection times.

As previously indicated, the hyperbolic traveltimes given by equation 1 and consequently also by equation 2 assume a constant near-surface velocity around the central ray position. This means that for all source and receiver pairs in the area of the image contribution of one central ray according to the traveltimes function (equation 2), the near-surface velocity is taken as constant. Furthermore, it is also assumed that all involved source receiver positions are on a horizontal line (flat acquisition line). In the case of marine data, the two requirements are easily met. For land data, however, the traveltimes need to be corrected to account for both lateral changes of the near-surface velocity and also topographic irregularities along the seismic line.

The ZO section simulated by the CRS-MZO formalism does not suffer from uncertainties in the near-surface velocity. In fact, even with wrong near-surface velocity values, the CRS-MZO imaging procedure produces accurate high-resolution time images (i.e., time imaging is solely dependent on traveltimes slopes and curvatures). However, if the extracted CRS attributes are used for velocity inversion, the near-surface velocities must be well determined, because accurate CRS parameters are needed for reliable estimation of the velocity model.

### OPTIMIZATION STRATEGY

Similar to the CRS stack method, the main problem to implement the CRS-MZO method is to determine the two NIP-wave parameters ( $\beta_0, R_{NIP}$ ) for each ZO point. This problem can be solved by applying optimization techniques using as objective function the coherency measure (semblance) of the signal amplitudes in prestack data along the stacking operator. In other words, the problem to be solved with the optimization algorithm is as follows, for each point  $P_0(x_0, t_0)$  of the ZO section to be simulated search for the two NIP-wave parameters ( $\beta_0, R_{NIP}$ ) which maximize the semblance condition. The convergence of the optimization process depends on the behavior of the objective function, that in most of the cases has one global minimum and more than one local minimum, i.e., the coherence measure of seismic signal is a multimodal function. Therefore, we have in many situations more than one minimum and we need to consider the global minimum and at least one local minimum to construct properly places of seismic events with conflicting dips.

To determine the NIP-wave parameters from the prestack data, we could use a similar multi-step search strategy as proposed in Jäger et al. (2001) to determine the three CRS parameters. But, in this work, to solve the two-dimensional global optimization problem to find the pair of parameters ( $\beta_0, R_{NIP}$ ) that produce the largest coherence value, we use a simulated annealing (SA) algorithm Corana et al. (1987). This optimization strategy uses multicoverage prestack seismic data as input and equation 2 to define the stacking surface. To start the SA algorithm, the SA algorithm uses random values generated from a priori defined intervals ( $90^\circ \geq \beta_0 \geq -90^\circ$  and  $0 < R_{NIP} < \infty$ ) into which the NIP-wave parameters will be searched. As result of this procedure, we obtain the optimized NIP-wave parameters for a given ZO point  $P_0(x_0, t_0)$ .

### CRS-MZO ALGORITHM

Based on the described global optimization strategy to search the NIP-wave parameters, we propose a three step algorithm to simulate a ZO section by CRS-MZO.

#### **Step I : Parameter search**

For one point  $P_0(x_0, t_0)$  of the ZO section to be simulated, at least one pair of NIP-wave parameters ( $\beta_0, R_{NIP}$ ) are searched from the multicoverage prestack seismic data of one super-bin by applying the described optimization strategy.

#### **Step II : CDS-MO-MM stack**

For one pair of NIP-wave parameters ( $\beta_0, R_{NIP}$ ) associated to the point  $P_0$ , a multi-offset (MO) and multi-midpoint (MM) stack along the CDS traveltimes from equation 2 is applied to the prestack data of the selected super-bin.

#### **Step III : CDS-ZO-MM demigration**

For the same pair of NIP-wave parameters  $(\beta_0, R_{NIP})$  associated to the point  $P_0$ , a ZO-MM demigration using the CDS traveltimes approximation from equation 2 with  $h = 0$  is applied on the stacked sample value, the result of step II.

In order to handle events with conflicting dips at point  $P_0$ , the steps II and III are repeated for all the remaining searched NIP-wave parameter pairs associated to that point. Finally, the search, the stack, and the demigration from the steps I, II, and III are repeated for all the remaining points  $P_0$  of the ZO section until the CRS-MZO section is complete.

## APPLICATION

To show the performance of the CRS-MZO approach, we apply it to the dataset of the simple synthetic model with homogeneous layers, separated by two smooth interfaces. The prestack data were generated using an acoustic finite difference code with absorbing boundaries in order to avoid generating surface related multiples. The dataset has 140 common shot sections each with 48 traces, and 25m interval between shots and receivers. The minimum and maximum offsets are 25m and 1200m, respectively. The time sampling interval is 4ms and the total record time is 2s. A small amount of white noise (5%) was added before applying any processing step. As a reference of comparison with our CRS-MZO imaging result we use the noise free modeled ZO section (Figure 4).

After searching for the NIP-wave parameters, we build a first image (shown in Figure 5) by applying solely step II of the CRS-MZO approach, the multi-offset-multi-midpoint stack (CDS-MO-MM) to all available super-bins. This section has obvious similarities with the well known CRS stacking method, clean section of accurately simulated ZO reflection events with some issues on resolving conflicting dips and diffraction events. The complete imaging result of the CRS-MZO approach is shown in Figure 6 after applying step II and step III, which is the multi-offset-multi-midpoint stack and the zero-offset-multi-midpoint demigration. Comparing this result with the modeled ZO sections, we observe that the CRS-MZO resolves better conflicting dips and strong diffractions by preserving the high quality character of CRS techniques.

To test the robustness of the CRS-MZO approach proposed in this paper, we applied it to the well-known Marmousi synthetic dataset (Bourgeois et al., 1991). The Marmousi experiment was computed on a model with highly complex structures and tectonically realistic distribution of reflectors, and it has strong velocity gradients in both vertical and horizontal directions. Therefore, this dataset is a great challenge for any imaging method based on hyperbolic moveout.

The CRS-MZO stack proposed here is fully automatic, namely no user interaction is required. In addition, the Marmousi multicoverage data was not submitted to any pre-processing before applying the CRS-MZO approach. Figure 7 shows the result of applying solely the CDS-MO-MM stack, and figure 8 shows the result of the complete CRS-MZO approach. Again, and more clearly visible, is the improved resolution of conflicting dips and strong diffractions after applying the complete CRS-MZO approach. For reasons of comparison, we processed the Marmousi data also running conventional NMO/DMO processing. This result is shown in Figure 9. By comparing the results, it is easily verified that the CRS-MZO stack (Figure 8) resolves better strongly dipping events especially in the deeper part of the Marmousi model. The CRS-MZO application shows also clearer events in the central and shallow part of the section at places where the NMO/DMO events are generally blurred. This provides a good indication that the CRS-MZO, which in contrast to NMO/DMO is valid for general heterogeneous media can help to improve the image in tectonically complex areas.

The CRS-MZO algorithm was also applied to line 50-RL-90 of the Tacutu Basin. This data is composed by 179 split-spread shot records, with an interval of 200 m and with 50 m receiver spacing. The nearest and farthest receivers are located at 150 m and 2500 m from the source, respectively. The record length is 4 seconds with a sample interval of 4 ms. Line 50-RL-90 is coarsely sampled in space, has a low signal to noise ratio, and with a nominal fold of 24 also a low data coverage, just to mention some of the processing challenges we had to deal with.

The following pre-processing sequence was applied: 1) trace editing; 2) geometry application; 3) spherical divergence correction; 4) deconvolution; and 5) F-K filtering for ground roll removal. Static corrections were not applied due to insufficient data information, which in this case of relatively smooth topography was not a severe problem. After applying the above pre-processing sequence, the data was stacked by using

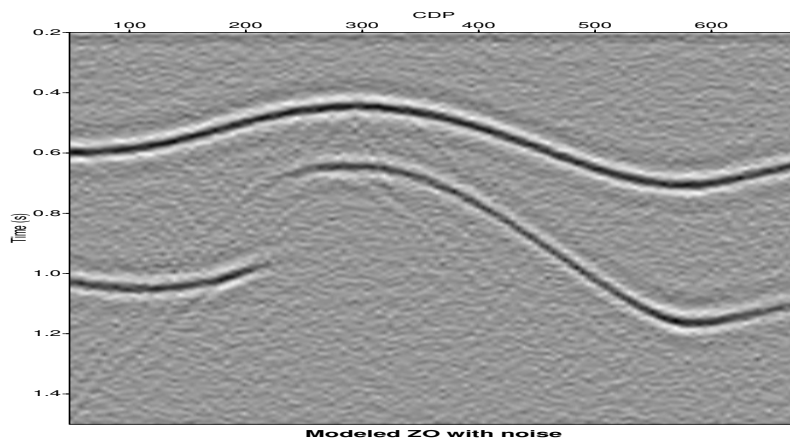


**Figure 4:** Modeled ZO section obtained by finite difference program for a simple synthetic model with two homogeneous layers above a half-space separated by curved interfaces. The second interface has two discontinuities

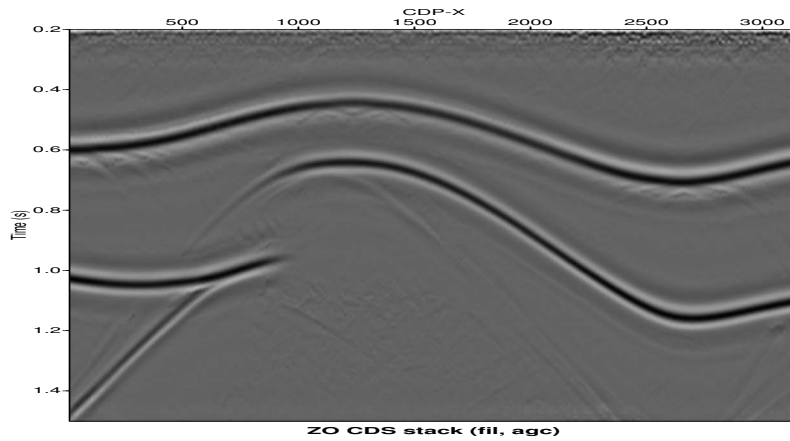


**Figure 5:** Simulated ZO stacked section obtained by the first step of the CRS-MZO approach applied to multicoverage data for simple synthetic model

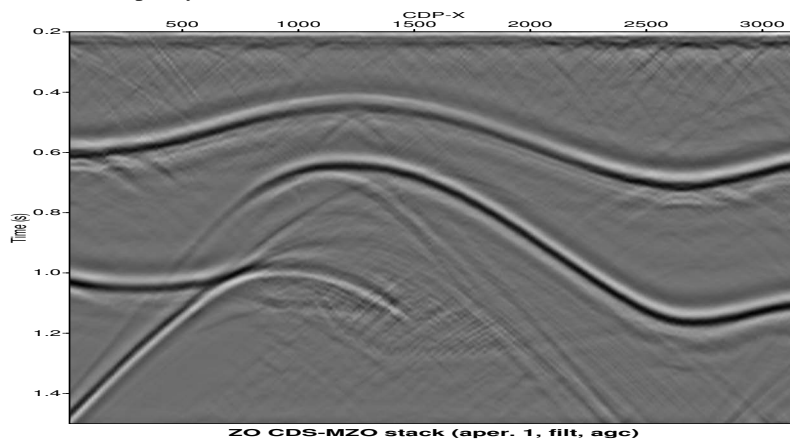


**Figure 6:** Simulated ZO stacked section obtained by the second step of the CRS-MZO approach applied to multicoverage data for simple synthetic model

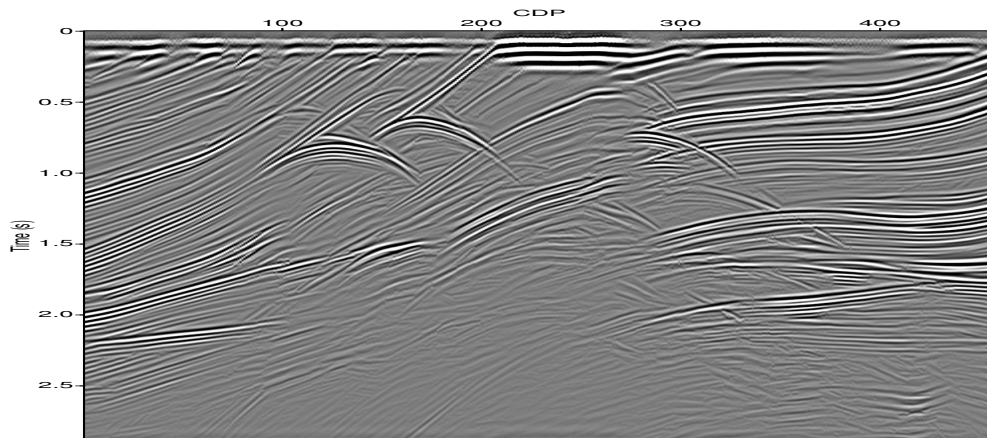


**Figure 7:** Simulated ZO section that result from the first step of the CRS-MZO approach applied Marmousi dataset.

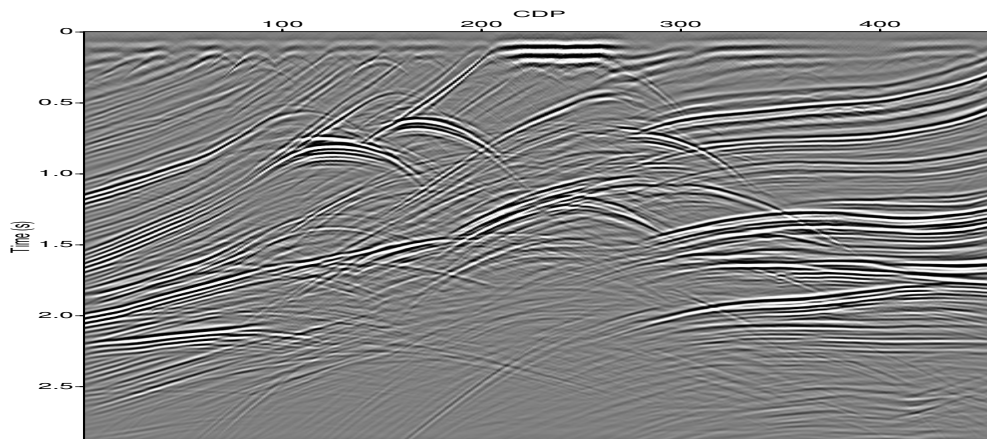


**Figure 8:** Simulated ZO section that result from the second step of the CRS-MZO approach applied Marmousi dataset.

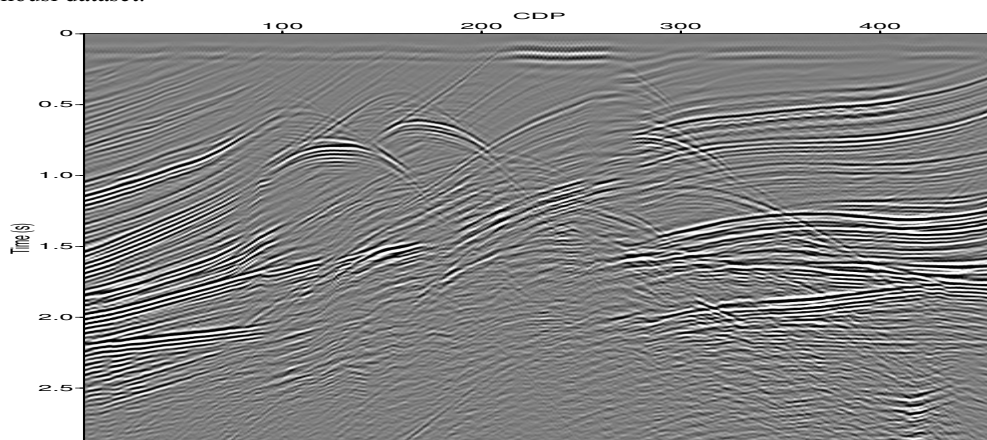


**Figure 9:** Simulated ZO section by the NMO/DMO stack method that result from the Marmousi dataset.

the CMP and the CRS approaches.

The CRS-MZO approach applied to line 50-RL-90, consisting of the three steps, Nip-parameter estimation, CDS-MO-MM stack, and CDS-ZO-MM demigration, is automatically performed. The image solely using the CDS-MO-MM stack is shown in Figure 10 and the complete result of the CRS-MZO application in Figure 11.

The corresponding CMP imaging approach consisting of: 1) velocity analysis, 2) NMO correction, 3) DMO correction, and 4) horizontal stack is shown in Figure 12.

Due to the coarse spatial sampling all images are deteriorated by aliasing, which makes the comparison between the different imaging approaches difficult. For instance, the highest dips in the shallow part, strongly emphasised by the CRS-MZO approach, are heavily affected by aliasing over the entire frequency bandwidth down to 15Hz. However, the CRS-MZO clearly performs better than NMO/DMO in the deep part of the section, showing a better continuity of the reflections and also a higher resolution.

## CONCLUSIONS

The CRS-MZO method is introduced as a multi-offset multi-midpoint diffraction stack followed by a zero-offset demigration. The diffraction stack and demigration operators are both derived from the general CRS formula by assuming diffraction points at the endpoints of the central rays. The CRS-MZO is like the CRS stack a fully automatic time imaging method. The needed imaging parameters are searched by a one-step search approach using a global optimization scheme.

CRS-MZO is, in contrast to DMO, valid for generally heterogeneous media. The robustness of this technique in complex media is demonstrated using the Marmousi model. The CRS-MZO shows a better continuity of strongly dipping events particularly in areas of abrupt lateral velocity variation.

Finally, we applied the CRS-MZO method to the field data, line 50-RL-90 of the Tacutu Basin. Due to the coarse spatial sampling, strong aliasing noise makes the comparison between the different imaging approaches difficult. However, the CRS-MZO clearly performs better than NMO/DMO in the deep part of the section, showing a better continuity of the reflections and also a higher resolution.

## ACKNOWLEDGMENTS

The first author thanks the National Petroleum Agency (ANP-Brazil) and the National Council for Scientific and Technological Development (CNPq-Brazil) for scholarships during his doctoral studies at the Federal University of Pará-Brazil. W.S. thank PGS for the permission to contribute to this development.

## REFERENCES

- Birgin, E. G., Biloti, R., Tygel, M., and Santos, L. (1999). Restricted optimization: a clue to a fast and accurate implementation of the common reflection surface stack method. *Journal of Applied Geophysics*, 42:143–155.
- Bourgeois, A., Bouget, M., Lailly, P., Poulet, M., Ricarte, P., and Versteeg, R. (1991). Marmousi, model and data. *52nd. EAGE mtg., Proceedings of the Workshop on Practical Aspects of Seismic Data Inversion*, pages 5–16.
- Chira-Oliva, P., Tygel, M., Zhang, Y., and Hubral, P. (2001). Analytic CRS stack formula for a 2D curved measurement surface and finite-offset reflections. *Journal of Seismic Exploration*, 10:245–262.
- Corana, A., Marchesi, M., Martini, C., and Ridela, S. (1987). Minimizing multimodal functions of continuous variables with 'Simulated Annealing' algorithm. *ACM Transactions on Mathematical Software*, 13(3):262–280.
- Garabito, G., Cruz, J. C., Hubral, P., and Costa, J. (2001). Common reflection surface stack: A new parameter search strategy by global optimization. *71th. Annual Meeting, SEG, Expanded Abstracts*.
- Garabito, G., Cruz, J. C., Hubral, P., and Costa, J. (2006). Depth mapping of stacked amplitudes along n attribute based zo stacking operator. *76th. Annual Meeting, SEG, Expanded Abstracts*, 2629–2632.

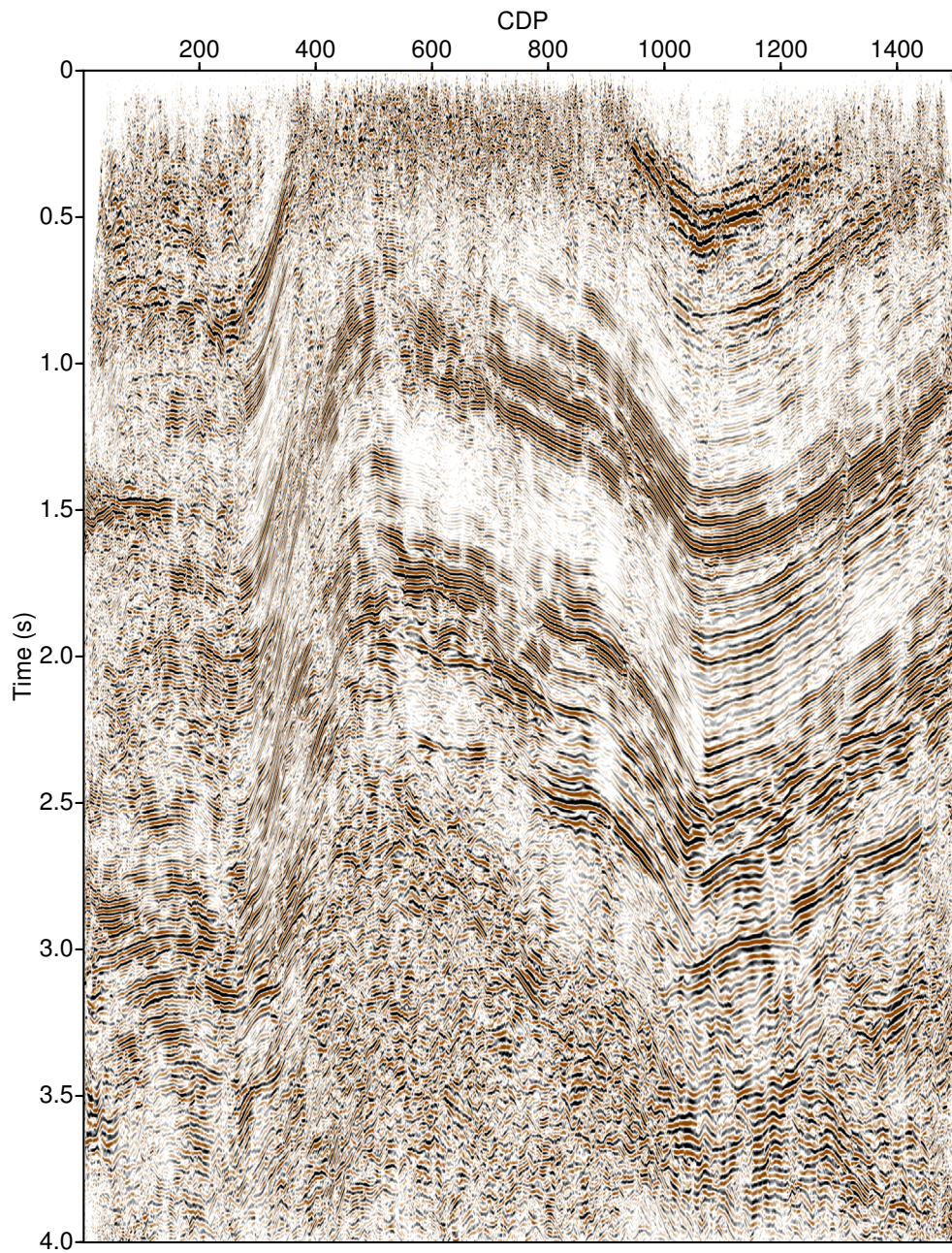


**Figure 10:** Simulated ZO section that result from the first step of the CRS-MZO approach applied to seismic line 50-RL-90 of the Tacutu Basin, Brazil.

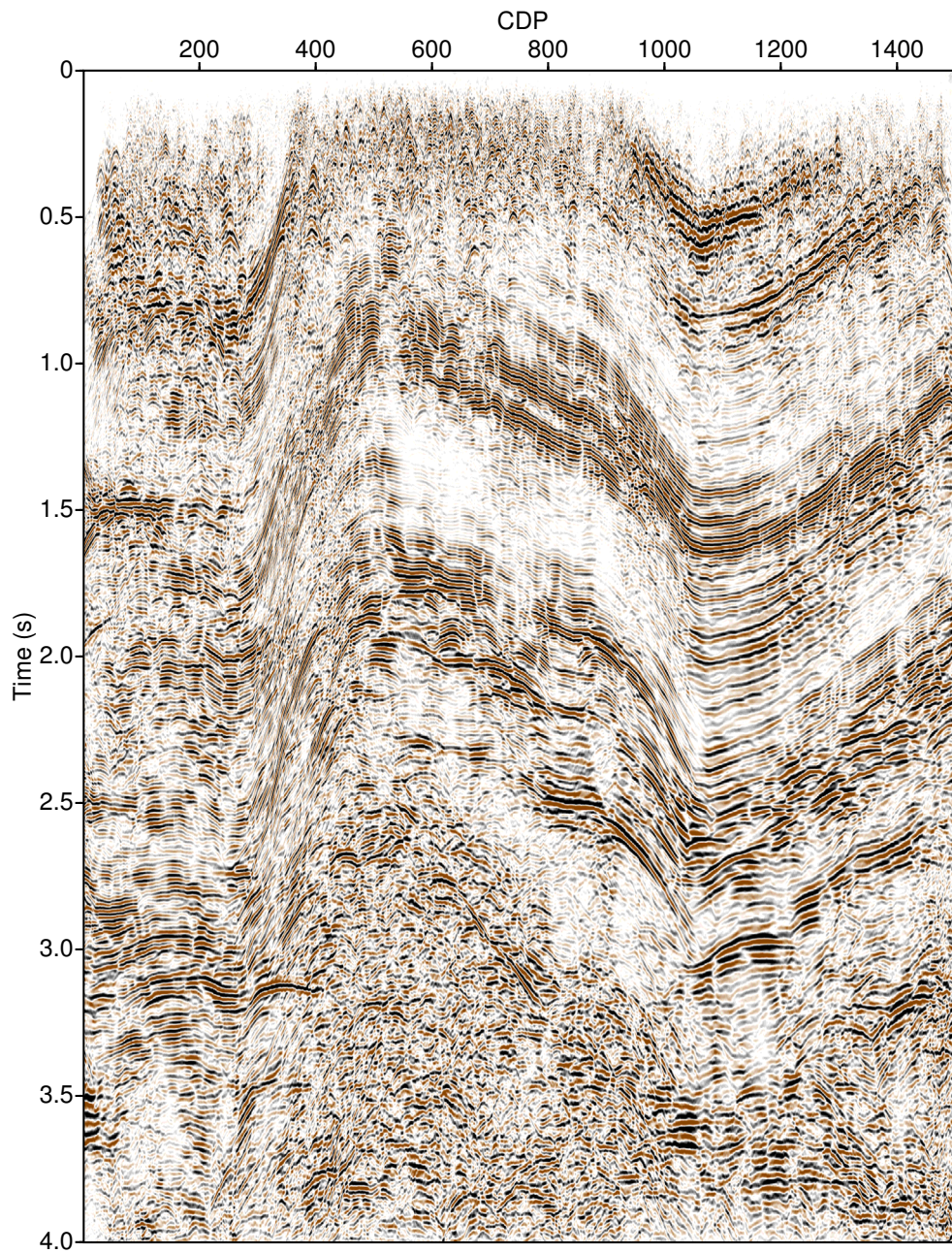


**Figure 11:** Simulated ZO section that result from the second step of the CRS-MZO approach applied to seismic line 50-RL-90 of the Tacutu Basin, Brazil.

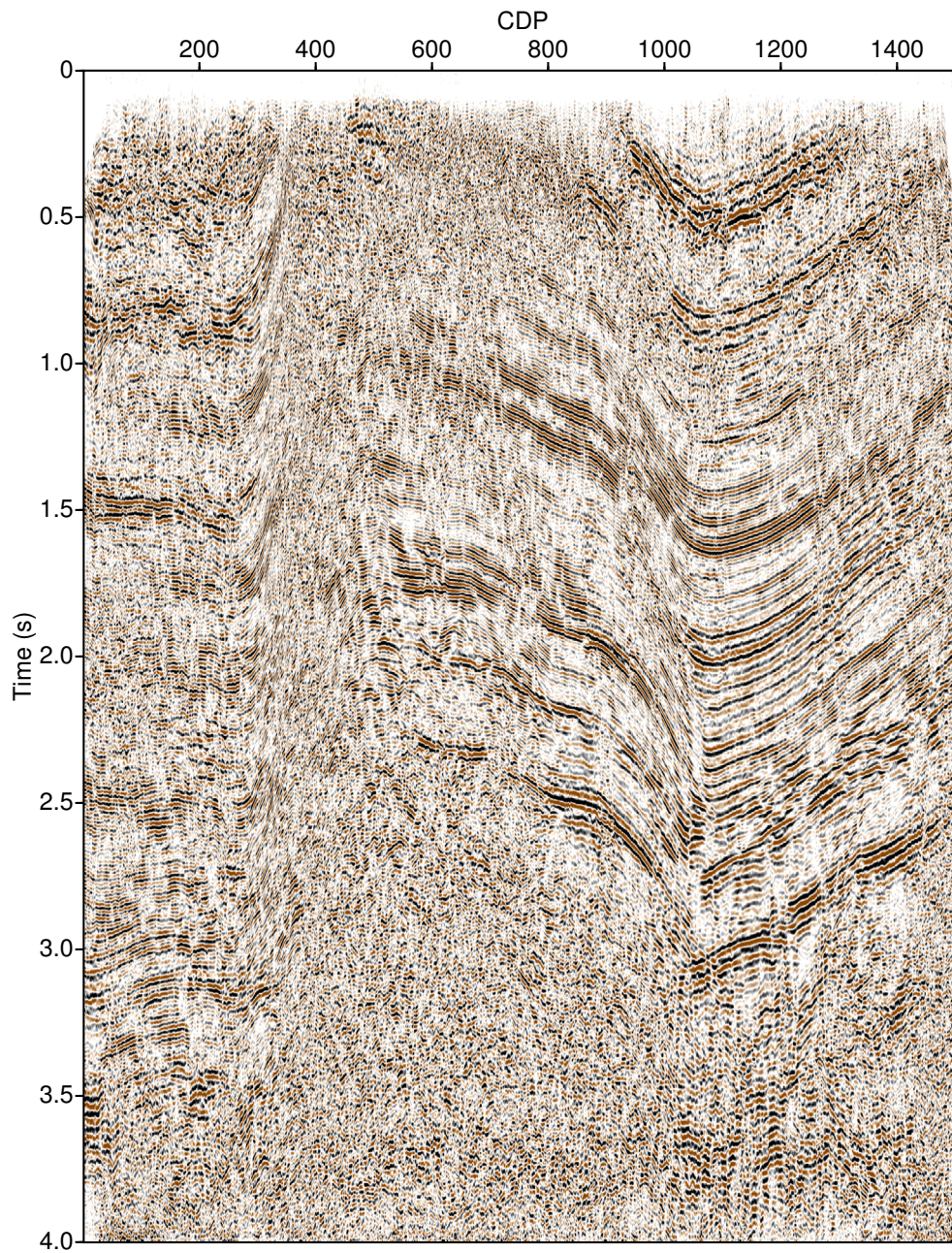


**Figure 12:** Simulated ZO section by NMO/DMO stack method applied to seismic line 50-RL-90 of the Tacutu Basin, Brazil.

- Hubral, P., Höcht, G., and Jäger, R. (1999). Seismic illumination. *The Leading Edge*, 18:1268–1271.
- Hubral, P. and Krey, T. (1980). Interval velocities from seismic reflection time measurements: Monograph. *Soc. Expl. Geophys.*
- Jäger, R., Mann, J., Höcht, G., and Hubral, P. (2001). Common reflection surface stack: Image and attributes. *Geophysics*, 66:97–109.
- Kirkpatrick, S., Gelatt, C., and Vecchi, M. (1983). Optimization by simulated annealing. *Science*, 220:671–680.
- Mann, J. (2001). Common-reflection-surface stack and conflicting dips. In *Extended Abstracts, 71th Annual Internat. Mtg., Expl. Geophys.*
- Mann, J., Hubral, P., Traub, B., Gerst, A., and Meyer, H. (2000). Macro-model independent approximative prestack time migration. *62th Mtg., Eur. Assoc. Expl. Geophys., Expanded Abstracts, Session B-5.*
- Müller, T. (1998). Common reflection surface stack versus nmo/stack and nmo/dmo/stack. *60th Mtg. Eur. Assoc. Expl. Geophys., Extended Abstracts.*
- Müller, T. (1999). The common reflection surface stack method - seismic imaging without explicit knowledge of the velocity model. *Ph.D. Thesis, University of Karlsruhe, Germany.*
- Schleicher, J., Tygel, M., and Hubral, P. (1993). Parabolic and hyperbolic paraxial two-point traveltimes in 3D media. *Geophys. Prosp.*, 41:495–513.
- Tygel, M., Müller, T., Hubral, P., and Schleicher, J. (1997). Eigenwave based multiparameter traveltime expansions. *Expanded Abstract of the 67th Annual Internat. Mtg., Soc. Expl. Geophys.*
- Zhang, Y., Bergler, S., and Hubral, P. (2001). Common-Reflection-Surface (CRS) stack for common-offset. *Geophys. Prosp.*, 49:709–718.